FACTA UNIVERSITATIS
Series: **Automatic Control and Robotics** Vol. 12, N° 2, 2013, pp. 103 - 119

DESIGN OF A MAXIMUM POWER POINT TRACKING CONTROLLER FOR A PV SYSTEM *

UDC (621.373+004.087.5):004.942

Miona Andrejević Stošović, Marko Dimitrijević

University of Niš, Faculty of Electronic Engineering, Department of Electronics, Niš, Serbia

Abstract. *In the first part of this paper, the photovoltaic (PV) panel-to-DC/DC converter interface will be studied experimentally and by simulation. Quantities will be defined to characterize the properties of the signals being DC with proper AC component due to the switching in the converter. In the second part an improved maximum power point tracking (MPPT) algorithm and also the results of its implementation into the standalone PV system were presented. Robustness of the improved MPPT algorithm will be studied regarding changes of the load to the converter and the illumination of the PV panel.*

Key words: *Modelling; Simulation; MPPT algorithm; MPPT controller; Output resistance*

1. INTRODUCTION

The benefits of solar energy usage include clean and sustainable electricity to the world while the carbon footprint of PV (photovoltaic) systems is decreasing every year. PV systems can provide clean power for large, as well as small applications. They are already installed and generating energy around the world on individual homes, housing developments, offices and public buildings.

The optimal design of modern PV oriented power systems as part of the Smart Grid concept [1], however, may be accomplished only by proper modelling and simulation of entire PV – electronic power system.

Our main interest in our previous work was to search for application of dynamic modelling of the PV system. A large set of published results was consulted, to mention only a few of them [2]–[7], and we came to a conclusion that no dynamic circuit modelling was

Received September 25, 2013
Corresponding author: Miona Andrejević Stošović
University of Niš, Faculty of Electronic Engineering, Department of Electronics, Aleksandra Medvedeva 14, 18000 Niš, Serbia•E-mail: miona.andrejevic@elfak.ni.ac.rs
* **Acknowledgement**. This research was partially funded by The Ministry of Education and Science of Republic of Serbia under contract No. TR32004 for the period 2011-2014.

exercised at all. In fact, under dynamic modelling of PV systems thermal transient analysis was understood.

Trying to establish some influence to the PV system design chain, in our recent proceedings [8], [9] we proved by simulation and measurements that the interface of the photovoltaic (PV) panel and the DC/DC converter is by no means a circuit with simple signals. Namely, as it is the case in the AC branch of the electricity distribution chain where the sinusoidal waveforms are distorted by nonlinear loads [10], here, due to the commutations within the converter, the current, or better to say, energy taken from the PV panel, is not constant and has a pulse shaped waveform. As a consequence, the current, voltage, and power waveforms at the PV panel's output have an AC component that is to be identified and its effects should be studied. Usually that interface is equipped by an electrolytic capacitor of a large capacitance that is supposed to short-circuit the AC component of the interface voltage. Its AC current sinking capacities, however, were shown to be limited and the AC component was not eliminated. Furthermore, real capacitors exhibit series resistance and inductance that influence the resulting voltage at the basic and harmonic frequencies of the main switches within the converter. It is needless to say that all – the capacitance, inductance, and resistance of the electrolytic capacitor are strongly temperature dependent and subject of aging. Altogether, because of the alternating component of the PV panel output voltage that comes from the converter, the PV-panel's working point is taken out of the maximum power point with high frequency and with amplitude that can reduce the output power, so in this paper we will present a control system that establishes maximum power.

After describing the measurements performed and results obtained, we will here create a simulation setup in order to generate quantitative characterization of the variables encountered at the PV-panel-converter interface. Quantities such as current and voltage ripple will be defined and calculated. Accordingly, power efficiency will be analysed and quantified.

The paper is organized as follows. The characterization of the system under consideration will be discussed first. Further, measurement and corresponding extracted data will be given. In the second and the third section DC and AC characterization of the PV panel will be deliberated. The interface will be characterized in the fourth section. Definitions will be introduced for quantities expressing the properties of the interface. Dependences of these quantities on the PV current will be extracted by simulation.

In the fifth section we will describe the most frequently used algorithm for MPPT named Perturb and Observe (P&O) as described in [7,8,9]. A minor improvement of the way how the algorithm is expressed will be introduced, leading to a Modified Perturb and Observe (MP&O) algorithm. This topic is presented in detail in [11]. Finally, in the sixth section, the MPPT system will be implemented in a standalone PV system, so the simulation results verifying the new algorithm reported will be introduced. For the first time, in this paper we will present how our control system behaves when output resistance of the whole PV system changes. We will show here that our system adjusts very well to resistance increase, as well as to its decrease.

2. DC CHARACTERIZATION OF THE PV SYSTEM

In this paper, a real system built of a solar panel, DC/DC converter, the MPPT subsystem and a resistive linear load will be considered. The system is schematically represented in Fig. 1.

Most of the parts of the PV system depicted in Fig. 1 are already modelled and simulated in SPICE e.g. [4-6]. There is no, however, published results reporting SPICE modelling and simulation of the MPPT circuit. By creation of such a model, we expect, one will be capable to simulate and design the whole standalone system, hence the importance of our work.

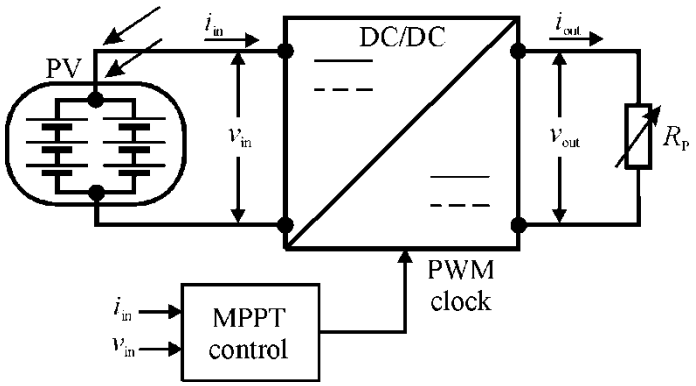

Fig. 1 Representation of the PV system to load connection

A function of a PV cell is simple: it converts the energy of light directly into electrical energy by the photovoltaic effect, first observed by E. Becquerel in 1839. When there is a load connected to the cell, electric current will flow, without any external voltage source. PV cells are based on a variety of light-absorbing materials, including mono-crystalline silicon, polycrystalline silicon, amorphous silicon, thin films such as cadmium telluride (CdTe) and copper indium gallium selenide (CIGS) materials, as well as organic/polymer-based materials.

The PV cells are connected together into columns (cells connected in series) and rows (columns connected in parallel) in order to get appropriate values of output voltage and current, respectively. The structure obtained is mounted on panels, hence the name. Fig. 2 depicts a typical DC characteristic of a small panel. Here the output current and power of the panel are shown as functions of the panel output voltage. MPP stands for Maximum Power Point.

The characterization of the system depicted in Fig. 1 was performed using a PV panel consisting of 18 cells connected in two equal columns. The Mean Well NSD15-S [12] converter was used. Resistor denoted by R_P was used as a variable load. Its lowest resistance values were limited by the modest driving capabilities of the DC/DC converter.

For characterization of the system the following dependences were measured as a function of the load resistance: the output DC current, the output DC voltage, the output DC power, the input DC power; providing possibility for converters efficiency to be computed.

The measurements are performed using PC running virtual instrument with National Instruments cDAQ-9174 USB chassis [13]. The chassis is equipped with two data acquisition modules: NI9225 and NI9227. NI9225 has three channels of simultaneously sampled voltage inputs with 24-bit accuracy, 50kSa/s per channel sampling rate and $300V_{RMS}$ range [14]. NI9227 is four channels input module with 24-bit accuracy, 50kSa/s per channel sampling rate, designed to measure $5A_{RMS}$ nominal and up to 14A peak on each channel [15].

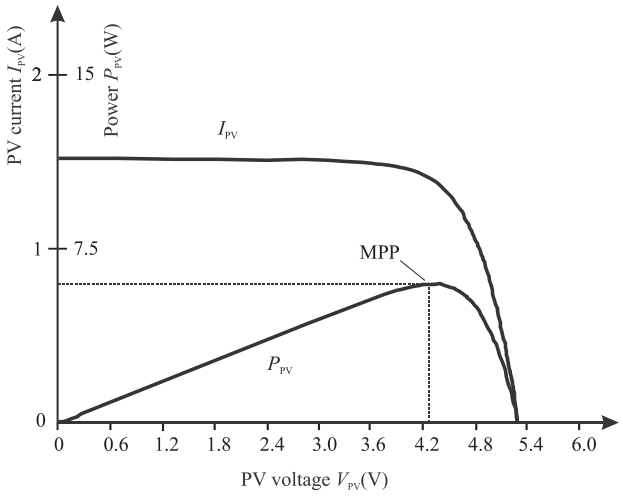

Fig. 2 Measured PV current and power as a function of the voltage of a PV cell

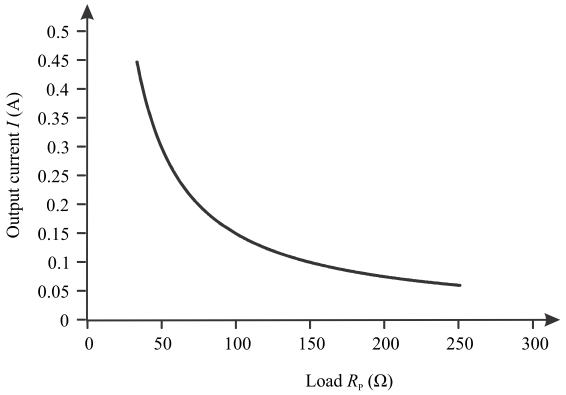

Fig. 3 The output DC current of the system as a function of the load to the system under full insolation

The voltages and the currents are sampled directly at the input and output points of the DC/DC converter (Fig. 1). Virtual instrument calculates power and power efficiency in real time, as well as other parameters that will be defined in this paper. It also performs

FFT analysis of sampled signals. Virtual instrument is implemented using National Instruments LabVIEW development package [16].

All these dependences are depicted in Fig. 3 – Fig. 5. The measurements were undertaken at noon of the (sunny) April 20, 2012. The panel was positioned for best incident angle of the incoming light. As it can be seen from the diagrams, the input voltage is practically independent of the load, while the input and the output power are decreased when the load resistance is raised. That, in a smaller scale, stands for the efficiency of the converter.

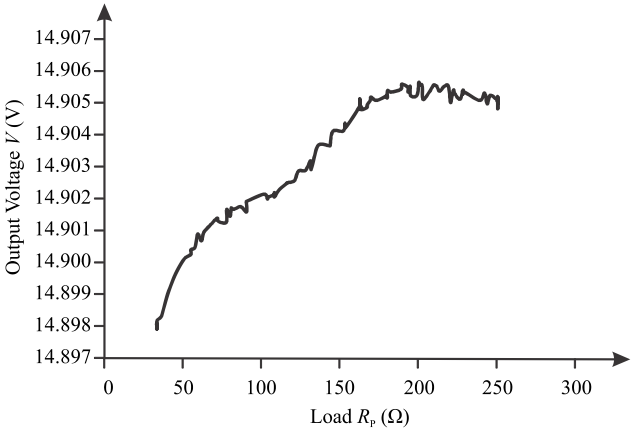

Fig. 4 The output DC voltage of the system as a function of the load to the system under full insolation

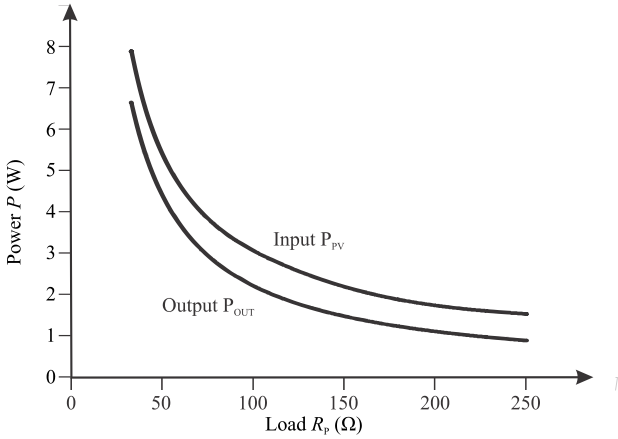

Fig. 5 Input and output DC power of the converter as a function of the load to the system under full insolation

3. DESCRIPTION AND AC CHARACTERIZATION OF THE PV PANEL

The fact of crucial importance for this paper is that when measurements with high insolations were done no alternating component of the panel's current and voltages were observed. That was in contrast to the expectations based on the results obtained by simulation.

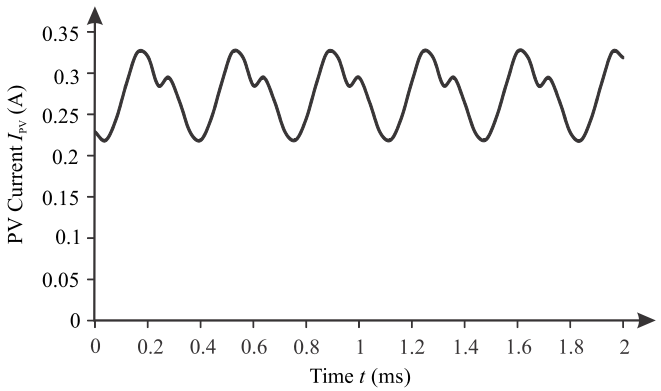

Fig. 6 PV panel's output and the inverter's input current as a function of time or measurement under cloudy weather, $R_P = 100\ \Omega$

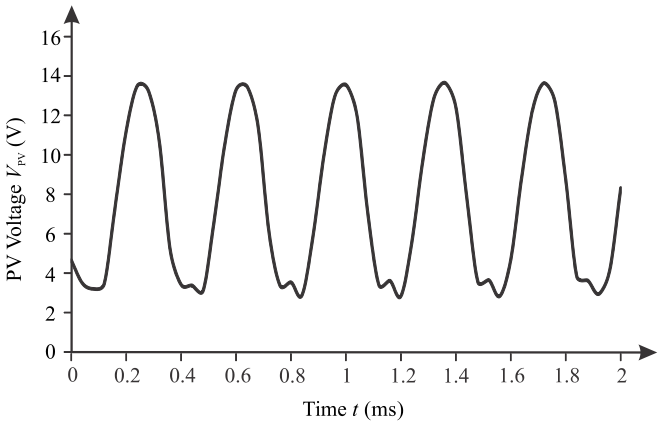

Fig. 7 PV panel's output and the inverter's input voltage as a function of time for measurement under cloudy weather, $R_P = 100\ \Omega$

New measurements were performed, however, in a cloudy day. Completely different results were produced by the absolutely same measurement setup. Namely, both the PV panel's current and voltage got a significant AC component due to the decrease of the photovoltaic current and the relative rise of its component that is driving the internal diode of every PV cell in the panel. In that way the output resistance of the PV panel is

raised and the converter currents produce a voltage drop on it that is time dependent. All this may be recognized from Fig. 6 and Fig. 7 where the measurement results are depicted. Fig. 6 represents the current that is leaving the PV panel and entering the converter as a function of time. As it can be seen, a considerable AC component with higher harmonics may be observed with the main constituent at the converters switching frequency.

Similarly, Fig. 7 represents the PV panel's output and the inverter's input voltage as a function of time for measurement under cloudy weather. Here again, significant AC component is observed. To quantify, Fig. 8 depicts the spectrum of the signal from Fig. 7. As it can be seen the DC component is only 12 dB larger than the first harmonic, while the rest of the harmonics are not easily negligible.

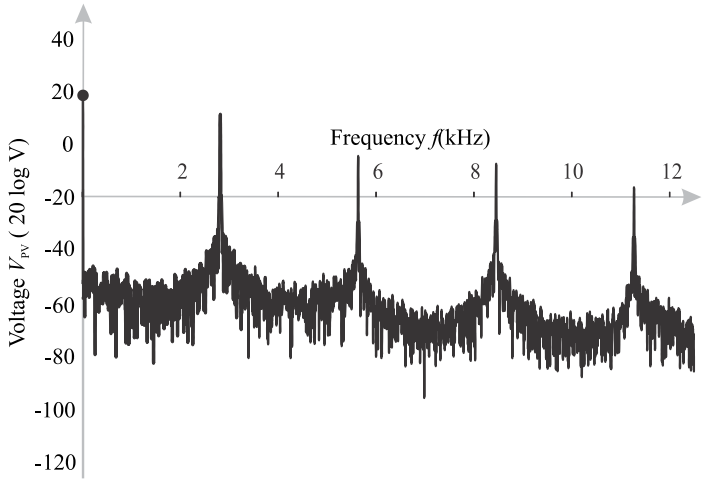

Fig. 8 Spectrum of the PV panel's output and the inverter's input voltage as a function of frequency for measurement under cloudy weather, $R_P = 100\Omega$

4. Quantification of the Properties of the PV Panel- Converter Interface

To get a realistic representation of the properties of the PV panel – converter interface we here introduce several definitions. In that way evaluation of the quality of the interface will be enabled. To do that we use the above mentioned panel. For a set of values of the photocurrent the optimum value of the duty cycle was adjusted to a value, so that the input resistance of the converter is equal to the equivalent output resistance of the solar panel at the MPP. For that value the voltage and current at the interface were produced by simulation in time domain.

A PV cell is usually modelled by a light-induced current source, I_P, in parallel with a diode. The output of the current source is proportional to the light flux falling onto the cell. The diode determines the I – V characteristics of the cell. Because of material defects and ohmic losses in the cell substrate material as well as in its metal conductors, surface, and contacts, the PV cell model also must include series and shunt resistance,

respectively, to account for these losses. The series resistance is a key parameter because it limits the maximum available power and the short-circuit current of the PV cell [2], [17].

Fig. 9 depicts the steady state current-voltage relationship for a large value of the photocurrent.

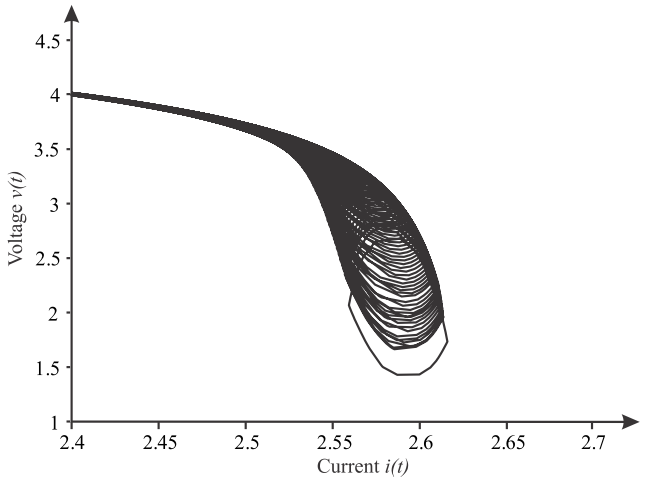

Fig. 9 Chaotic diagram representing the current voltage relationship at the PV panel - converter interface for I_P = 1.3A

Similarly, Fig. 10 represents the average value of the instantaneous power in steady state. Based on these simulations the following is introduced.

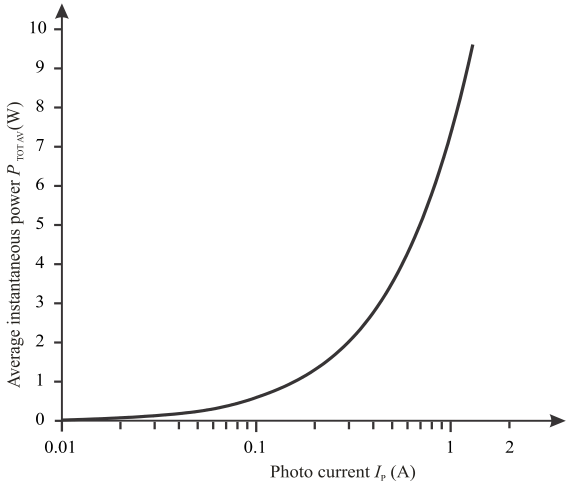

Fig. 10 Average value of the instantaneous power in steady state at MPP as a function of irradiation (here represented by the photocurrent)

Let the measured waveforms at the PV panel-converter interface be the voltage $v(t)$ and the current $i(t)$.

The DC components of the voltage and current are calculated as:

$$V_{\mathrm{DC}} = \frac{1}{k\mathrm{T}} \int_{\tau}^{\tau+k\mathrm{T}} v(t)\,\mathrm{d}t \tag{1}$$

and

$$I_{\mathrm{DC}} = \frac{1}{k\mathrm{T}} \int_{\tau}^{\tau+k\mathrm{T}} i(t)\,\mathrm{d}t \tag{2}$$

Here k is to be kept as small as possible. It would be the best to have k=1 but since the sampling usually does not match exactly the period, to reduce the numerical error, one should use a slightly larger value, k=3 for example.

The voltage ripple factor is defined as

$$r_v = 100 \cdot V_{\mathrm{AC\,m\,TOT}} / V_{\mathrm{DC}}\,[\%], \tag{3}$$

where $V_{\mathrm{AC\,m\,TOT}} = \sqrt{\sum V_{\mathrm{AC\,m}i}^2}$, while V_{ACmi} is the amplitude of the i^{th} harmonic of $v(t)$. As the first harmonic is the one having the frequency of the switching signal, only the first harmonic is taken into consideration.

Similarly the current ripple factor is determined as

$$r_i = 100 \cdot I_{\mathrm{AC\,m\,TOT}} / I_{\mathrm{DC}}\,[\%], \tag{4}$$

where $I_{\mathrm{AC\,m\,TOT}} = \sqrt{\sum I_{\mathrm{AC\,m}i}^2}$, while $I_{\mathrm{AC\,m}i}$ is the amplitude of the i^{th} harmonic of $i(t)$. The dependence of r_{v} and r_{i} on the photocurrent under optimal power transfer conditions is depicted in Fig. 11.

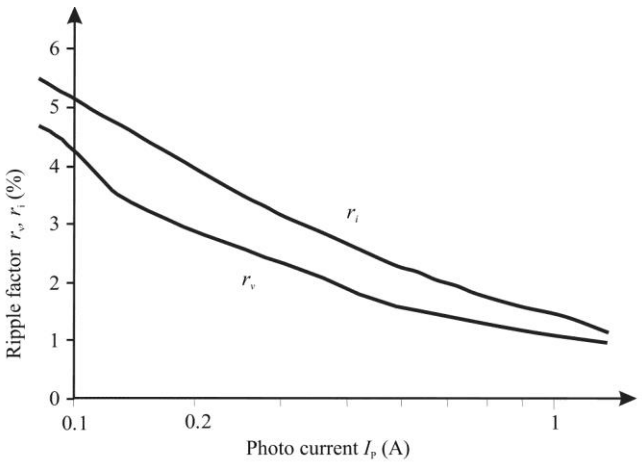

Fig. 11 The voltage ripple factor (r_v), the current ripple factor (r_i), of the PV-panel as a function of irradiance. MPP (optimum duty cycle) kept for every value of I_P.

The average of the total power is obtained from:

$$P_{\text{TOT AV}} = \frac{1}{k\text{T}} \int_{\tau}^{\tau+k\text{T}} v(t) \cdot i(t)\, \text{d}t \tag{5}$$

while the DC power is

$$P_{DC} = I_{DC} \cdot V_{DC}. \tag{6}$$

Fig. 10 depicts $P_{\text{TOT AV}}$ as a function of the illumination. The residue is defined by the difference:

$$P_{\text{RES TOT}} = P_{\text{TOT AV}} - P_{\text{DC}} \tag{7}$$

This will be referred to as residual total power. This is an important quantity representing the energy oscillating between the PV panel and DC/DC with no positive effects on the energy balance.

The AC components of the voltage and current at the PV panel-converter interface are defined as

$$v_{\text{AC}}(t) = v(t) - V_{\text{DC}} \tag{8a}$$

$$i_{\text{AC}}(t) = i(t) - I_{\text{DC}} \tag{8b}$$

These definitions allow for computation of the average power related to the AC components only:

$$P_{\text{AC}} = \frac{1}{kT} \int_{\tau}^{\tau+kT} v_{\text{AC}}(t) \cdot i_{\text{AC}}(t)\, \text{d}t. \tag{9}$$

It will be referred to as AC power. Substituting $v_{\text{AC}}(t)$ and $i_{\text{AC}}(t)$ from (8a) and (8b) into equation (9) implies:

$$P_{\text{AC}} = P_{\text{TOT AV}} - \frac{V_{\text{DC}}}{kT} \int_{\tau}^{\tau+kT} i(t)\, \text{d}t - \frac{I_{\text{DC}}}{kT} \int_{\tau}^{\tau+kT} v(t)\, \text{d}t + P_{\text{DC}} \tag{10a}$$

leading to:

$$P_{\text{AC}} = P_{\text{TOT AV}} - P_{\text{DC}} = P_{\text{RES TOT}}. \tag{10b}$$

Having this result in mind, from now on, the AC power will be used only as the quantity defining energy balance.

The AC power factor is:

$$\eta_{\text{AC}} = 100 \cdot P_{\text{AC}} / P_{\text{tot av}} [\%]. \tag{11}$$

The dependence of this quantity on the photocurrent is depicted in Fig. 12. One may observe that the largest value is obtained at very low illumination. Note the absolute value is small, almost negligible, what is a consequence of the fact that P_{AC} is obtained as a product of the AC components that constitute small amount of their DC counterparts as can be seen from Fig. 12. Its value for ideal conditions should be zero.

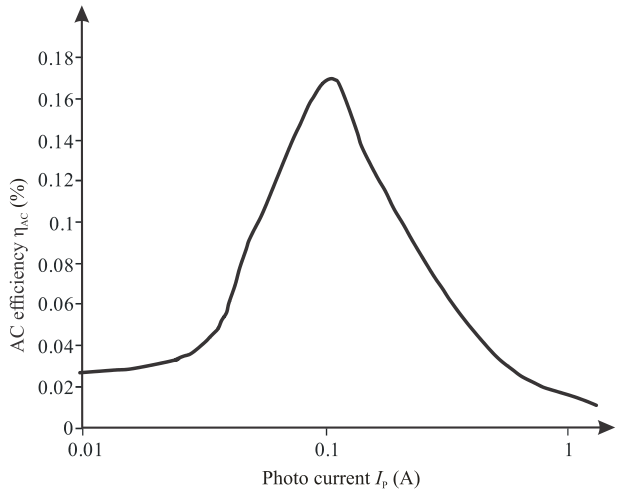

Fig. 12 η_{AC} as a function of I_P at MPP

Finally, we define the balance factor as:

$$\varepsilon = 1 - P_{AC} / P_{DC}. \tag{12}$$

Its value under ideal conditions should be equal to unity.

5. MPPT ALGORITHMS

All previous calculations and dependences were done under one condition: MPP (maximum power point, i.e. optimum duty cycle) kept for every value. Keeping MPP at optimum value would be easy if there are no reasons for maximum power point migration during the operation of the PV system.

But, it can be shown that MPP migrates slightly due to the change of the output resistance of the panel [18]. Also, there exists the migration of the MPP with changes of the temperature [19]. Due to these reasons every PV system is equipped with a specific circuitry which controls the duty cycle of the pulse train controlling the switches within the converter (inverter). These changes lead to changes of the input resistance of the converter and if the control is properly tailored the PV panel will be kept in a position to deliver maximum power to the converter.

There are several techniques and algorithms in the literature enabling implementation of the idea of tracking the MPP. Among them the most popular is the so called Perturb and Observe (P&O) which is depicted in Fig. 13 [20, 21]. It can be seen from the Fig. 13 that as a result a fixed increment of the PV panel voltage is produced after each sampling period. This increment is actually used to forward information to a pulse width modulated oscillator in order to control its duty ratio.

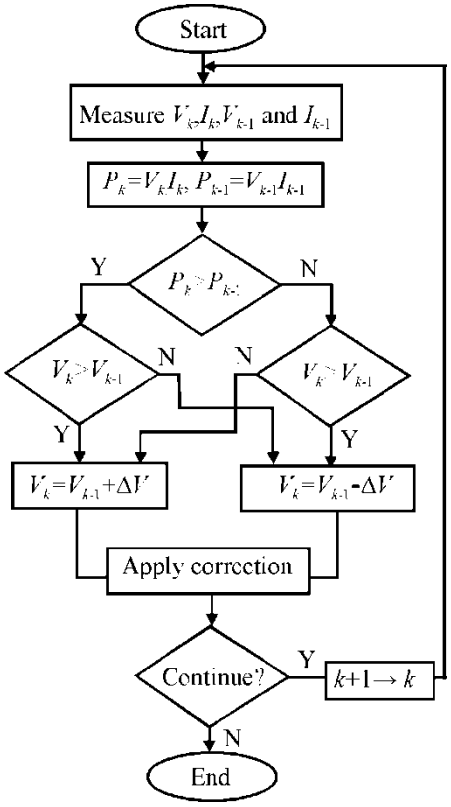

Fig. 13 The perturb and observe algorithm

There exist four branches in this algorithm leading to different signs of the increment: positive or negative. In the cases: (P_k–P_{k-1}>0 & V_k–V_{k-1}>0) and (P_k–P_{k-1}<0 & V_k–V_{k-1}<0) the increment is positive. The value of the increment is negative if (P_k–P_{k-1}<0 & V_k–V_{k-1}>0) and if (P_k–P_{k-1}>0 & V_k–V_{k-1}<0). These two statements imply that the sign of the increment is in fact associated to the sign of Q_k=(P_k–P_{k-1})*(V_k–V_{k-1}). If Q_k>0 the increment is positive and if Q_k<0 the increment is negative. This conclusion simplifies the whole diagram and the electronic circuitry implementing the algorithm.

We can notice that this algorithm is generating an increment no matter how large the differences (P_k–P_{k-1}) and (V_k–V_{k-1}) are, what, generally speaking, for small differences, may lead to a change in the duty cycle that is larger than necessary, what can even become counterproductive leading the quiescent point out of MPP region.

If we consider this disadvantage of the algorithm, we will try to find a better solution, so we propose a modification of the previously described algorithm, depicted in Fig. 14. In this algorithm, after calculation of Q_k, we first make a comparison with a threshold value Q_{ref}. If |Q_k| is not larger than Q_{ref} there is no need for change of the duty cycle.

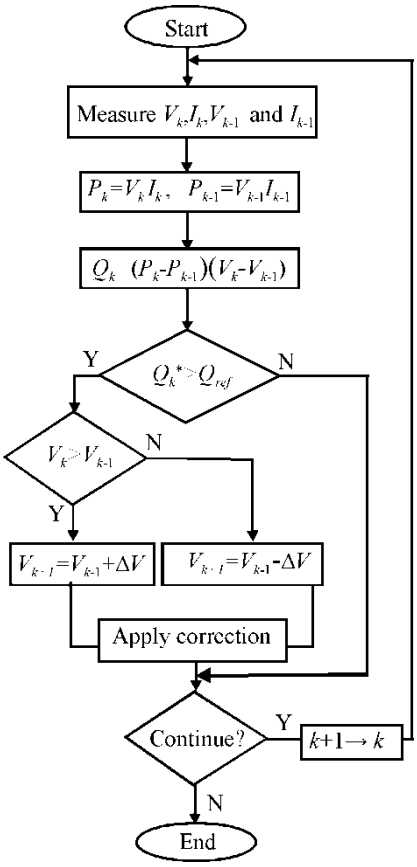

Fig. 14 The modified perturb and observe algorithm

But, if it is larger, the sign of Q_k is used to determine the sign of the voltage increment.

The implementation of this idea is leading to one more benefit: by proper choice of Q_{ref} and ΔV, larger voltage increments may be implemented, i.e., we can expect faster recovery of the MPPT.

6. Implementation into the System and Simulation Results

The SPICE implementation of the algorithm in Fig. 14 is given in [11]. We will not describe its realization here in a detail because this was previously done, but we will concentrate to its implementation in a complete PV system and the results of this implementation.

In Fig. 15 we can see the pulse width modulated signal that is in fact output of our MPPT system. That is the signal that defines the switching frequency of the converter. We notice from the figure that its width is 0.65 (pulse width is $1.3*10^{-5}$s, and the period is $2*10^{-5}$s), and this is the optimal width for the case when input photocurrent is 1.3A. For some other illumination, the pulse width is different, what is in fact the goal of the system- to produce the pulses controlling the system, so the system reaches maximum power.

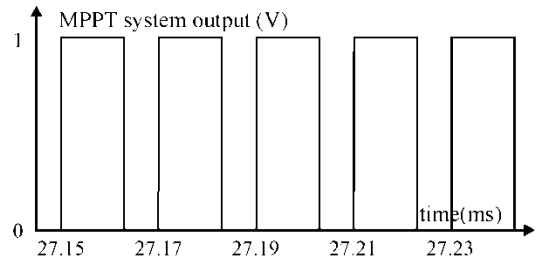

Fig. 15 Pulse width modulated signal at the output of MPPT system

In the Fig. 16 we can see the instantaneous power at the panel-converter interface for that case (when input photocurrent is 1.3A), and we checked using simulations and calculations that it is really maximum power (9.6W) for that value of illumination.

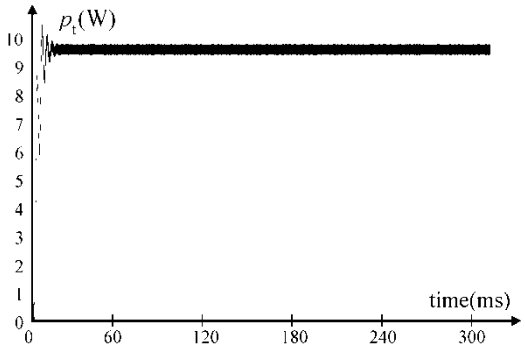

Fig. 16 Instantaneous power at the panel-converter interface for I_P = 1.3A

For other illumination value (when input photocurrent is 0.6A) we also checked the system, and we can see results in Fig. 17. We also obtained maximum power for that value of illumination.

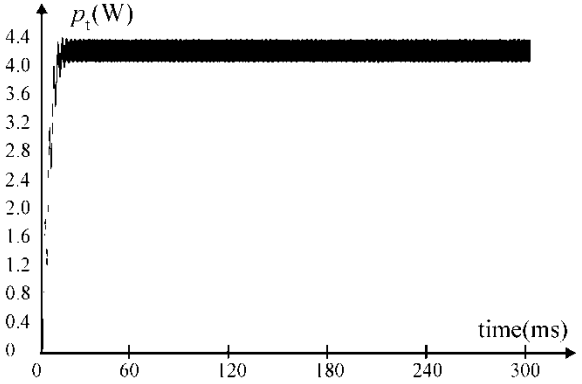

Fig. 17 Instantaneous power at the panel-converter interface for I_P=0.6A

Further, we examined our system operation in the situation, when there is a change of the output resistance. As it may be seen the MPP migrates slightly due to the change of the output resistance of the panel [17].

From the Fig. 18, we can see that when output resistance is decreased (10% - from 115.5Ω to 104Ω), the power also decreases. The value of 115.5Ω is adjusted so the system produces maximum power. With another output resistance, the MPPT migrates, so the power at the panel-converter interface decreases. The value of that power cannot increase for any change in the system because its maximum value is for the output resistance value of 115.5Ω.

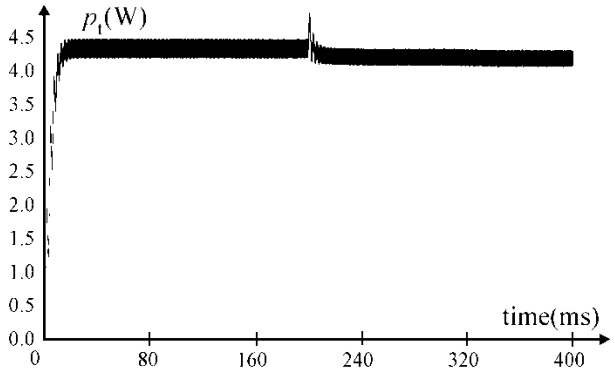

Fig. 18 Instantaneous power at the panel-converter interface when R_P changes from 115.5Ω to 104Ω (I_P=0.6A)

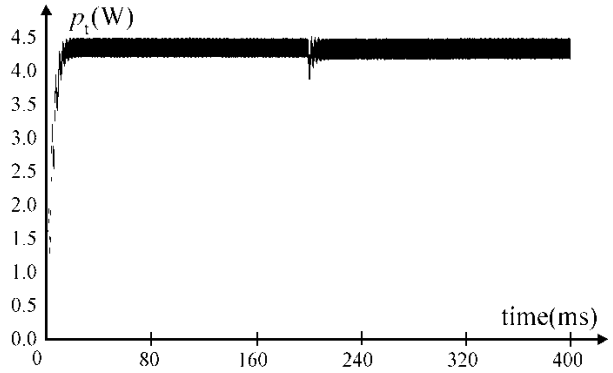

Fig. 19 Instantaneous power at the panel-converter interface when R_P changes from 115.5Ω to 127Ω (I_P=0.6A)

In Fig. 19, we checked the output resistance increase (also 10%), and the situation is similar. There is a slight change of the power, but it decreases again, what was expected.

Finally, in Fig. 20 we present a situation when the output resistance is dramatically decreased (from 115.5Ω to 50Ω), so the power decrease is evident because of the system disorder.

From the last three figures we can conclude that our system behaves correctly in the situations when output resistance is from some reason changed.

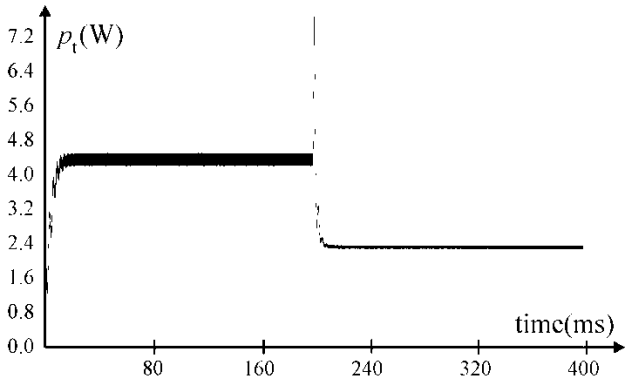

Fig. 20 Instantaneous power at the panel-converter interface when R_P changes from 115.5Ω to 50Ω (I_P=0.6A)

7. CONCLUSION

After characterization of the PV system and panel-converter interface, we demonstrated improvement of the MPPT algorithm in this paper. Then we considered its implementation into the PV system. Simulation results show that MPPT controller shows good results in obtaining maximum power at the panel-converter interface, for the optimum value of the output resistance, as well as when the output resistance dynamically changes.

REFERENCES

[1] L. Cepa, Z. Kocur, Z. Muller, "Migration of the IT technologies to the smart grids," Electronics and Electrical Engineering, vol. 18, no. 7, pp. 123–128, 2012. [Online]. Available: http://dx.doi.org/10.5755/j01.eee.123.7.2390

[2] G. H. Yordanov, O. M. Midtgård, "Physically-consistent parameterization in the modeling of solar photovoltaic devices," in *Proceedings of Power Technology*, Trondheim, Norway, pp. 1–4, 2011. [Online]. Available: http://dx.doi.org/10.1109/PTC.2011.6019232

[3] K. Leban, E. Ritchie, "Selecting the accurate solar panel simulation model," in *Proceedings of Nordic Workshop on Power and Industrial Electronics*, Helsinki, Finland, pp. 1–7, 2008.

[4] H. I. Cho, S. M. Yeo, C. H. Kim, V. Terzija, Z. M. Radojević, "A steady-state model of the photovoltaic system in EMTP," in *Proceedings of International Conference on Power Systems Transients* (*IPST2009*), Kyoto, Japan, Session 7A - Distributed Generation, Paper 20, 2009.

[5] H. L. Tsai, C. S. Tu, Y. J. Su, "Development of generalized photovoltaic model using MATLAB/-SIMULINK," in *Proceedings of the World Congress on Engineering and Computer Science*, San Francisco, USA, pp. 846–851, 2008.

[6] M. Azab, "Improved circuit model of photovoltaic array," International Journal of Electrical Power and Energy Systems Engineering, vol. 2, no. 3, pp. 185–188, 2009.

[7] T. O. Saetre, O. M. Midtgård, G. H. Yordanov, "A new analytical solar cell I-V curve model," Renewable Energy, vol. 36, no. 8, pp. 2171–2176, 2011. [Online]. Available: http://dx.doi.org/10.1016/j.renene.2011.01.012

[8] M. Andrejević Stošović, D. Lukač, V. Litovski, "Realistic modeling and simulation of the PV system - converter interface," in *Proceedings of the 4th Small Systems Simulation Symposium*, Niš, Serbia, pp. 28–32, 2012.

[9] M. Dimitrijević, M. Andrejević Stošović, Z. Petrušić, D. Lukač, "Experimental characterization of the PV panel - converter interface," in *Proceedings of the LVI Conference of ETRAN*, Zlatibor, Serbia, EL 4.3, 2012.

[10] T. Vaimann, J. Niitsoo, T. Kivipold, T. Lehtla, "Power quality issues in dispersed generation and smart grids," Electronics and Electrical Engineering, vol. 18, no. 8, pp. 23–26, 2012. [Online]. Available: http://dx.doi.org/10.5755/j01.eee.18.8.2605

[11] M. Andrejević Stošović, M. Dimitrijević, D. Lukač, V. Litovski, "Spice modeling and simulation of a MPPT algorithm," in *Proceedings of LVII Conference of ETRAN*, Zlatibor, Serbia, EL 1.4, 2013.

[12] Mean Well, "Mean Well NSD15-S – 15W regulated single output DC/DC," Available at http://www.meanwell.com/search/nsd15-s, 2013.

[13] National Instruments, "NI cDAQ-9174 NI CompactDAQ 4-slot USB chassis," Available at http://sine.ni.com/nips/cds/view/p/lang/sr/nid/207535, 2013.

[14] National Instruments, "NI 9225 operating instructions and specifications," Available at http://www.ni.com/pdf/manuals, 2013.

[15] National Instruments, "NI 9227 operating instructions and specifications," Available at http://www.ni.com/pdf/manuals, 2013.

[16] National Instruments, "LabVIEW system design software," Available at http://www.ni.com/labview, 2013.

[17] M. Andrejević Stošović, D. Lukač, I. Litovski, V. Litovski, "Frequency domain characterization of a solar Cell", in *Proceedings of 11th Symposium on Neural Network Applications in Electrical Engineering - NEUREL*, pp. 259–264, 2012. [Online]. Available: http://dx.doi.org/10.1109/NEUREL.2012.6420031

[18] M. Andrejević Stošović, M. Dimitrijević, D. Lukač, V. Litovski, "Quantification of power quality issues at the PV panel-converter interface," in *Proceedings of the IX Symposium on Industrial Electronics, INDEL 2012*, Banja Luka, Bosnia and Herzegovina, pp. 256–262, 2012.

[19] V. Salas, E. Olías, A. Barrado, A. Lázaro, "Review of the maximum power point tracking algorithms for stand-alone photovoltaic systems," Solar Energy Materials and Solar Cells, vol. 90, no. 11, pp. 1555–1578, 2006. [Online]. Available: http://dx.doi.org/10.1016/j.solmat.2005.10.023

[20] T. Esram, P. L. Chapman, "Comparison of photovoltaic array maximum power point tracking techniques," IEEE Transactions on Energy Conversion, vol. 22, no. 2, pp. 439–449, 2007. [Online]. Available: http://dx.doi.org/10.1109/TEC.2006.874230

[21] C. S. Chin, M. K. Tan, P. Neelakantan, B. L. Chua, K. T. K. Teo, "Optimization of partially sShaded PV array using fuzzy MPPT," *IEEE Colloquium on Humanities, Science and Engineering Research, CHUSER 2011*, Penang, China, pp. 481–486, 2011.